Journal of Oil Palm Research
DOI: https://doi.org/10.21894/jopr.2024.0041

SEPARATION AND THERMAL MODIFICATION OF MONTMORILLONITE FROM TANAH DATAR CLAY AND ITS CATALYTIC APPLICATION IN BIODIESEL PRODUCTION FROM WASTE FRYING OILS

ZARNIDA WIDIA NENGSIH[1]; RAHAYU RAHAYU[1]; SYUKRI ARIEF[1]; UPITA SEPTIANI[1]; MATLAL FAJRI ALIF[1] and SYUKRI SYUKRI[1]*

ABSTRACT

Natural clay comprises a blend of diverse minerals exhibiting distinct structures and characteristics. Montmorillonite exhibits strong acidity and stabilising effects on active species due to its unique layered structure, thus making it a suitable material for use as a heterogeneous catalyst. Therefore, this research aims to examine the effect of separation and thermal modification process of Tanah Datar clay minerals, as well as their catalytic activity in the conversion of waste frying oil (WFO) into biodiesel. The catalysts were evaluated using X-ray Diffraction (XRD), X-ray Fluorescence (XRF), and Laser Particle Size Analyser (LPSA). The uncalcined clay primarily consists of montmorillonite, along with kaolinite, hematite, and quartz. Upon calcination, montmorillonite transforms into meta montmorillonite. The particle size of montmorillonite increases after separation and calcination. The catalysts were employed in a lab-scale biodiesel production via transesterification reaction, employing a mole ratio of oil and methanol of 1:6, catalyst amount of 3% (w/w), stirring speed of 500 rpm, and a temperature of 70°C for 3 hr. Both uncalcined and calcined montmorillonite catalysts can enhance biodiesel yield by up to 80.11%. This observation demonstrates the considerable potential of the implemented treatment as a catalyst in biodiesel production.

Keywords: biodiesel, catalyst, clay, montmorillonite, transesterification.

Received: 27 November 2023**; Accepted:** 20 June 2024**; Published online:** 2 September 2024.

INTRODUCTION

Energy is one of the factors in sustaining human life activities. Energy consumption always increases every year. Continuous energy use results in a shortage of energy originating from fossil fuels. The use of fossil fuels is also a global problem due to excessive levels of CO_2 emissions, environmental impacts, and threats to the economy, environment, and human welfare (Azni *et al.*, 2023; Rehman *et al.*, 2021). One renewable energy source that can lessen the scarcity of fossil fuels and lessen environmental pollution is biodiesel (Pacheco-López *et al.*, 2021; Pikula *et al.*, 2020). Biodiesel fuel can replace fossil fuels used for diesel engines. It is more attractive than diesel fuel because it is non-toxic, biodegradable, and can be produced from renewable sources, making it a sustainable alternative fuel (Nguyen *et al.*, 2023; Siddeg *et al.*, 2022). Additionally, it can also help reduce greenhouse gas emissions by up to 86% compared to petroleum diesel (Suwarno *et al.*, 2021; Xu *et al.*,

[1] Chemistry Department,
Faculty of Mathematics and Natural Sciences,
Universitas Andalas, Limau Manis Campus,
Padang, 25163 Indonesia.

* *Corresponding author e-mail: syukridarajat@sci.unand.ac.id*

2022). It can be made through several methods, such as dilution, pyrolysis, microemulsion, and transesterification (Irawan *et al.*, 2021; Mishra and Goswami, 2018; Supriyanto *et al.*, 2021). The transesterification method is preferred for biodiesel due to its low cost compared to other methods. In addition, the transesterification process is also relatively simple (Gouran *et al.*, 2021; Salaheldeen *et al.*, 2021).

Making biodiesel by transesterification method uses raw materials containing triglycerides, such as vegetable oils. Some types of vegetable oils that have been used are sunflower (Jabbari, 2018; Khan *et al.*, 2023; Vital-López *et al.*, 2023), castor oil (Bibin *et al.*, 2020; Mustafa *et al.*, 2023; Ubaid *et al.*, 2022), coconut oil (Bambase *et al.*, 2021; Lugo-Méndez *et al.*, 2021), and palm oil (Nang *et al.*, 2009; Palaniselvam, 2023; Syukri *et al.*, 2022). However, the use of waste frying oil (WFO) is of great interest. This is because biodiesel from WFO is an environmentally friendly process. After all, WFO can be utilised, making it more economical and effective in waste management (Gouran *et al.*, 2021; Sukkathanyawat and Wichianwat, 2023). The transesterification reaction also requires a catalyst. The catalysts used can be homogeneous catalysts and heterogeneous catalysts. Homogeneous catalysts have disadvantages such as difficulty in catalyst separation, high effluent generation (Pasae *et al.*, 2021; Silva *et al.*, 2015), and equipment corrosion, while heterogeneous catalysts offer advantages like reusability, selectivity, and low cost (Faruque *et al.*, 2020; Gaide *et al.*, 2023; Kibar *et al.*, 2023). Therefore, many heterogeneous catalysts are now developed in the transesterification reaction, one of which is montmorillonite.

Montmorillonite belongs to the smectite group and has a 2:1 layer structure (Belghazdis and Hachem, 2022; Uddin, 2018; Yaghmaeiyan *et al.*, 2022). Alumina and silica make up the majority of montmorillonite, a typical cationic clay; other metal oxides make up a small portion (Tripol'Skaya *et al.*, 2009). Montmorillonite exhibits strong acidity and a stabilising effect on active species, such as metal nanoparticles, due to its unique layered structure. This makes it a suitable material for use as a heterogeneous catalyst (Takabatake and Motokura, 2022). Several studies have used montmorillonite as a catalyst for transesterification reactions, such as montmorillonite KST in producing biodiesel from palm oil (Kansedo *et al.*, 2009), the novel modified montmorillonite to produce biodiesel from castor and *Jatropha* oil (Negm *et al.*, 2017), and barium-loaded montmorillonite for the synthesis of biodiesel from waste cooking oil (WCO) (Sharma and Bhavani, 2021). Each of these reactions produces high yields of biodiesel. However, the chemical modification given to the montmorillonite catalyst requires complicated steps and is expensive (Shapkin *et al.*, 2017). Meanwhile, physical modifications can also be given to montmorillonite, such as thermal modifications (Abdrakhimova and Abdrakhimov, 2007; Wu *et al.*, 2022). Previous researchers reported that clay calcined at 850°C could increase biodiesel yield (Admi *et al.*, 2022).

The montmorillonite that is widely used in catalyst application is synthetic montmorillonite, which consequently increases production costs.. However, montmorillonite is one of the minerals contained in natural clay. Separating montmorillonite from natural clay can be a solution to reduce catalyst production costs. Montmorillonite was separated from Boyolali natural clay by previous researchers and applied as an oil-bleaching agent (Taslimah *et al.*, 2008). However, montmorillonite, separated from natural clay has never been used as a catalyst. Therefore, this research applies montmorillonite separated from natural clay as a catalyst in the transesterification reaction. Based on data in 2021, the availability of clay in Indonesia is very abundant. There are about 10 387.209 million tonnes of natural clay available in West Sumatera Province. Therefore, the catalyst raw material used in this study was taken from one of the areas in West Sumatera Province, namely Tanah Datar Regency because there have been no reports regarding the separation of montmorillonite minerals from clay in that area. The Tanah Datar area has abundant clay, which is characterised by the presence of brick production sites.

This study aims to determine the effect of separation process and thermal modification on mineral composition, physical and chemical properties of minerals, and catalytic activity of uncalcined and calcined montmorillonite from Tanah Datar clay in the process of converting WFO into biodiesel.

MATERIALS AND METHODS

Materials Preparation

The clays used in this study were taken from Andaleh, Batipuh District, Tanah Datar Regency, West Sumatra Province, Indonesia. The area is located at latitude 0°27'12.4"S and longitude 100°26'09.7"E in the form of a plateau area at an altitude of 946 m above sea level. The map of natural clay (*n-clay*) sampling locations can be seen in *Figure 1*. The *n-clay* was soaked in distilled water for 24 hr, filtered, and dried at 105°C for 3 hr. The clay was crushed and sieved with a sieve of 90 µm (Syukri *et al.*, 2020). The heated clay (*h-clay*) catalyst was obtained ready to be separated from the montmorillonite mineral. The transesterification reaction was carried out following the methods

reported by previous researchers (Fifi *et al.*, 2023) with some modifications using three times WFO and methanol (Merck) as raw materials. Ammonia hydroxide (NH_4OH) was used as a dispersing agent for montmorillonite from Tanah Datar clay following the method reported by previous researchers (Taslimah *et al.*, 2008).

Separation and Thermal Modification of Montmorillonite

Montmorillonite was separated by dispersing it in an NH_4OH solution. In brief, 25 g of *h-clay* was stirred in 400 mL NH_4OH 2% (v/v) with a magnetic stirrer for 15 min and left for two days (Taslimah *et al.*, 2008). The suspension was separated by centrifugation at 1000 rpm for 5 min. The precipitate was separated and dried in an oven at 105°C to obtain the montmorillonite clay (*Mt-clay*) catalyst. Thermal modification is carried out by calcining the *Mt-clay* catalyst at a temperature of 850°C in a furnace for 4 hr to obtain the calcined montmorillonite clay (*c-Mt-clay*) catalyst.

Catalyst Characterisation

The catalyst's crystallinity was assessed through the utilisation of X-ray Diffraction (XRD) equipment by X'Pert MPD (PANanalytical) which employed Cu Kα1 radiation (λ = 1.54059 Å). The equipment operated at 40 kV and 30 mA, covering an angular range of 2θ 10° to 90°. The oxide composition was determined using X-ray Fluorescence (XRF) equipment by NEXCG Rigaku. Particle size was assessed using the Laser Particle Size Analyser (LPSA) equipment by Labtron, LLPA-C10, which has a measuring range of 0.01-2000.00 µm.

Preparation and Determination of Free Fatty Acids in WFO

The preparation of WFO is done by heating it at 105°C until the water bubbles disappear. Free fatty acid (FFA) content was determined following the acid-base titration method reported by previous researchers (Febrianto *et al.*, 2020) with the Equation (1):

$$\% \ FFA = \frac{V_{NaOH} \times N_{NaOH} \times Bm_{fatty\ acid}}{M \times 1000} \quad (1)$$

where V_{NaOH} is the volume of 0.1 N NaOH titration (in mL), N_{NaOH} is normality of NaOH, $Bm_{fatty\ acid}$ is molecular weight of fatty acid (in g), and M is mass of oil sample.

Biodiesel Production Through Transesterification Reaction and Its Characterisation

The WFO used in this study has a density of 0.90 g cm^{-3} and FFA of 1.65%. The FFA value is lower than 3% so WFO can be used directly in the transesterification reaction. Each catalyst was used in the transesterification reaction of WFO by refluxing method. The molar ratio of WFO and methanol used was 1:6 with 3% (w/w) catalyst. The transesterification reaction was carried out for 3 hr at 70°C with a stirring speed of 500 rpm. The catalyst and glycerol were separated from the product mixture by centrifugation. The biodiesel layer was washed with 50°C aquadest at a volume of 1:1 and homogenised for 5 min. The mixture was allowed to stand so that the dense water would separate as the bottom layer and drained out. The remaining water in the biodiesel was removed

Figure 1. Map of natural clay sampling locations.

using anhydrous Na_2SO_4. The yield of biodiesel was calculated using the Equation (2) (Munir *et al.*, 2019):

$$\% \text{ Yield} = \frac{\text{Mass of biodiesel produced (g)}}{\text{Mass of oil used (g)}} \times 100 \quad (2)$$

Product Analysis

The type and content of methyl esters produced in biodiesel products are identified using Gas Chromatography-Mass Spectrometry/GC-MS (Shimadzu QP 2010 Ultra). The GC-MS instrument is equipped with a DB5 MS column with Helium as a carrier gas and an injection temperature of 250°C. The biodiesel product was determined for density at 15°C (ASTM D6751) and moisture content (ASTM D2709).

RESULTS AND DISCUSSION

X-ray Diffraction Characterisation

Figure 2 shows the X-ray diffraction pattern of the *h-clay*, *Mt-clay*, and *c-Mt-clay* catalysts scanned at 2θ from 20°-90° that the Tanah Datar clay contains the minerals montmorillonite and kaolinite. The presence of montmorillonite (RRUFF ID: 110052) was found to have diffraction intensities at 2θ: 19.9° and 34.9°. Kaolinite in the *h-clay* sample was confirmed based on Inorganic Crystal Structure Database (ICSD) No. 68698 with the appearance of diffraction intensity at 2θ: 12.3°; 24.8°; 36.5°; 38.3°; 42.4°; 45.8°; 54.8°; and 62.3°. The presence of quartz (ICSD No. 68698) was found with high intensity at 2θ: 26.6°. Quartz is a stable phase of silica in the form of an inert compound. When at normal temperature, quartz has a trigonal quartz (α-quartz) structure (Götze *et al.*, 2021). The diffraction intensity of hematite (ICSD No. 154191) was also found at 2θ: 33.1°; 36.5°; 64.0°; and 75.7°.

The separation can cause changes in mineral peaks. Montmorillonite peaks appear at 2θ: 21.5° and 54.2°. Meanwhile, the peak that existed before separation remained after separation and there was an increase in intensity, namely at 19.9° and 34.9°. Kaolinite mineral as an impurity in *Mt-clay* also causes the disappearance of the peak at 2θ: 36.5°; 42.4°; 45.8°; and 54.8°. Meanwhile, the kaolinite peak that is still present in the *Mt-clay* sample has a low intensity at 2θ: 12.4°; 25.1°; 35.9°; and 62.4°. Hematite also experiences peak loss at 2θ: 36.5° and 75.7°. The thermal modification given to *c-Mt-clay* caused the disappearance of most of the montmorillonite mineral peaks (*Figure 2*). Montmorillonite peaks were only found at 2θ: 54.2° and 72.5° with very low intensity. The diffraction peaks of *c-Mt-clay* are dominated by hematite peaks, at 2θ: 24.3°; 33.2°; 41.0°; 49.6°; 62.7°; and 64.4°. Another interesting point is the appearance of a quartz peak at 2θ: 26.6° albeit with very low intensity, which was previously missing in the *Mt-clay* sample.

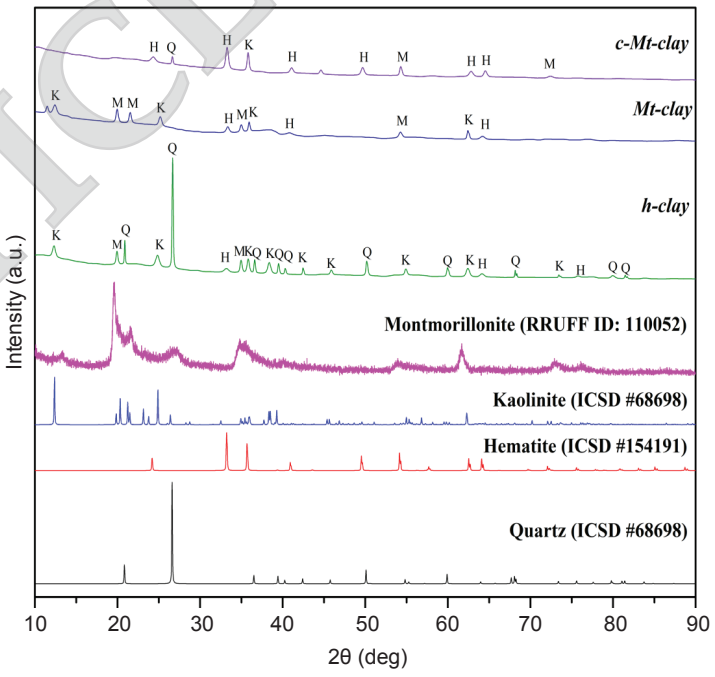

Note: M- montmorillonite, K- kaolinite, Q- quartz, H- hematite.

Figure 2. XRD diffratograms of h-clay, Mt-clay, *and* c-Mt-clay.

X-Ray Fluorescence Characterisation

Thermal separation and modification affect the elemental and oxide composition of each catalyst (*Table 1*). According to the XRF analysis, it is evident that all catalyst samples contain a significant proportion of silicon (Si) and aluminium (Al) elements in their composition, whose levels reach more than 60% of the total of all elements in the sample. This shows that the catalysts used are indeed classified as clay because they have the main constituent composition of clay (Lomertwala *et al*., 2019). In addition, it can be seen that the type of montmorillonite contained in Tanah Datar clay is Ca-montmorillonite because there is Ca content in the clay (Park *et al*., 2016). Iron oxide occupies the third highest position as a constituent composition of clay catalysts whose levels reach 19%-32%. Determination of the Si/Al mole ratio on the clay catalyst also needs to be done to determine the potential of the sample as a catalyst. It is known that the *h-clay* has a Si/Al mole ratio of 1.79; *Mt-clay* has a Si/Al mole ratio of 1.27; and *c-Mt-clay* has a Si/Al mole ratio of 1.26.

Laser Particle Sizer Analyser Characterisation

The particle size distribution of *h-clay* and *Mt-clay* catalysts may change due to the montmorillonite and separation process (*Figure 3*). The *h-clay* catalyst is significantly distributed at a particle size of 5.21 μm, accounting for 3.5% of the total samples. After separation and calcination, the particle size distribution increased to 9.6 μm for 4.37% of *Mt-clay* and to 37.86 μm for 9.37% of *c-Mt-clay*. This causes the specific surface area of particles (S) to decrease due to the separation and calcination process, where the known S values of *h-clay*, *Mt-clay,* and *c-Mt-clay* are 5.57 $m^2\ g^{-1}$, 1.73 $m^2\ g^{-1}$, and 0.24 $m^2\ g^{-1}$ (*Table 2*). *H-clay* has a particle size distribution of <0.1-2000.0 μm. While the particle size of *Mt-clay* and *c-Mt-clay* spread over >0.1-2000.0 μm.

The separation and calcination can cause the standard percentile value of the sample to rise (*Table 2*). The D10 of *h-clay* (0.51 μm) increased in *Mt-clay* (1.54 μm) and *c-Mt-clay* (13.01 μm). This shows that 10% of the samples are below 0.51, 1.54, and 13.01 μm in size. The D50 value of *h-clay* (4.74 μm) increased at *Mt-clay* (9.14 μm) and *c-Mt-clay* (33.01 μm). This indicates that 50% of the samples are smaller than this value for each sample. Similarly, the D90 value becomes 44.14, 54.37, and 83.72 μm in *h-clay*, *Mt-clay,* and *c-Mt-clay* which means that 90% of the samples have a small size of that value. The Dav (average particle size) value also increased in *h-clay* 20.75 μm to 23.94 μm in *Mt-clay* and 43.02 μm in *c-Mt-clay*. The increase in particle size on the catalysts after separation and calcination may be due to Van der Waals forces increasing the ability for particles to gather to form agglomerations (Hamed *et al*., 2019).

Mechanism for Separating Montmorillonite from Natural Clay

Montmorillonite mineral was separated from *h-clay* by dispersing it in an NH_4OH solution (Taslimah *et al*., 2008). NH_4^+ ions from NH_4OH enter the interlayer of montmorillonite minerals through interlayer cation exchange events, causing swelling in the montmorillonite structure (Gautier *et al*., 2010; Tong *et al*., 2021). Swelling that occurs due to intercalation by NH_4^+ ions can cause the

TABLE 1. CHEMICAL COMPOSITION OF *H-CLAY*, *MT-CLAY*, AND *C-MT-CLAY*

Oxide	*h-clay* (%)	*Mt-clay* (%)	*c-Mt-clay* (%)
Al_2O_3	22.854	22.893	25.845
SiO_2	48.356	34.459	38.502
P_2O_5	3.325	3.261	2.912
K_2O	1.108	0.743	0.599
CaO	0.677	0.688	0.597
TiO_2	2.122	1.866	1.777
V_2O_5	0.069	0.096	0.089
Fe_2O_3	20.476	32.657	28.606
ZnO	0.068	0.119	0.099
SrO	0.005	0.003	0.000
ZrO_2	0.076	0.101	0.066
Ag_2O	0.632	0.675	0.0682
PbO	0.014	0.032	0.024
Si/Al ratio	1.790	1.270	1.260

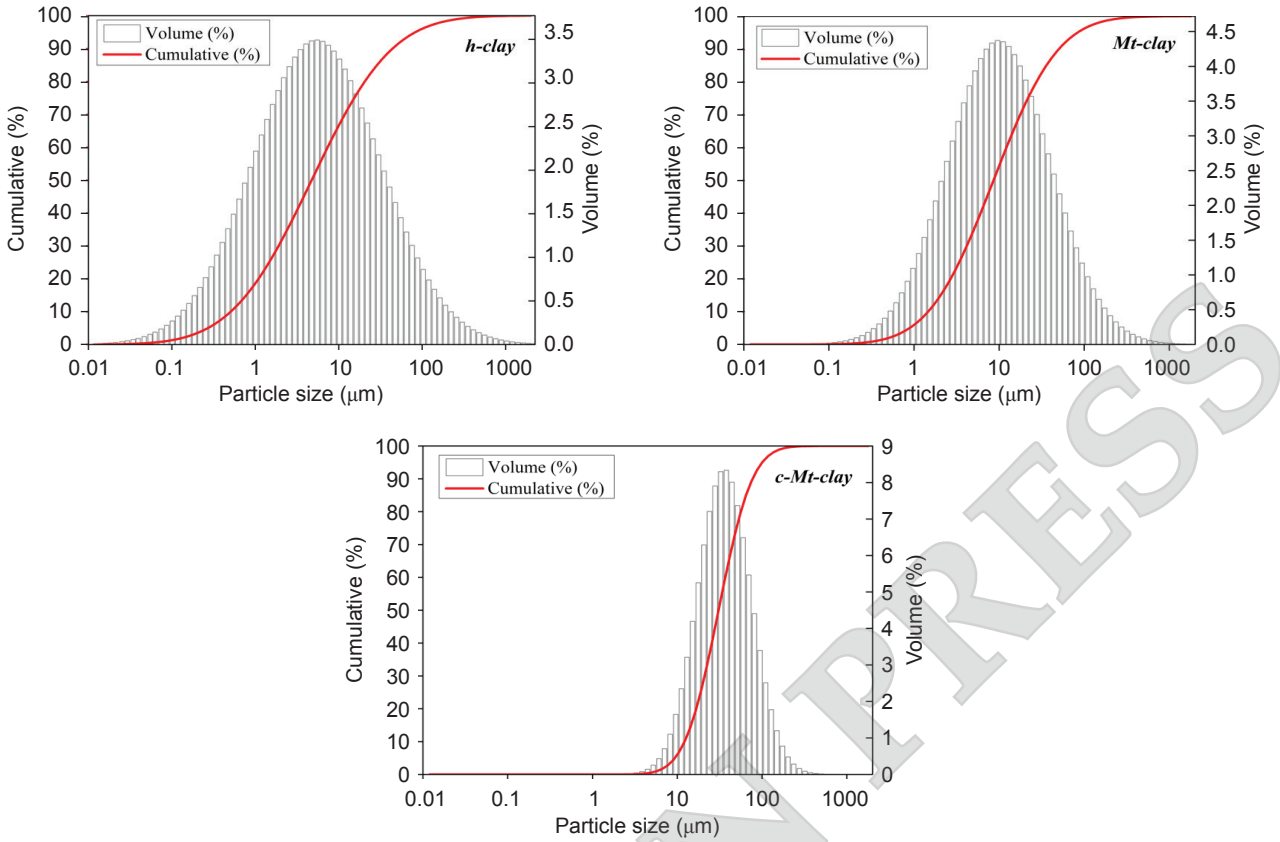

Figure 3. Particle size distribution curves of h-clay, Mt-clay, *and* c-Mt-clay.

TABLE 2. PARTICLE SIZE DISTRIBUTION CHARACTERISTICS OF *h-clay*, *Mt-clay*, AND *c-Mt-clay*

Type of catalyst	D10 (μm)	D50 (μm)	D90 (μm)	Dav (μm)	S ($m^2 g^{-1}$)
h-clay	0.51	4.74	44.14	20.75	5.57
Mt-clay	1.54	9.14	54.37	23.94	1.73
c-Mt-clay	13.01	33.01	83.72	43.02	0.24

Note: D10, D50, D90 - standard percentiles; Dav - average particle size (agglomeration size); S - specific surface area of particles.

opening of interlayer space in the montmorillonite structure. The distance between the layers of the montmorillonite structure will increase and eventually release so that the montmorillonite can be dispersed in the NH_4OH solution. In addition, the interaction of NH_4^+ ions with montmorillonite can also increase hydration in montmorillonite (Peng *et al.*, 2020). The separation mechanism of montmorillonite using NH_4OH solution can be seen in *Figure 4*.

Effect of Separation and Thermal Modification on Mineral Type and Composition

Separation of montmorillonite from *h-clay* has a significant effect on increasing the purity of *Mt-clay*. According to the XRD results, new montmorillonite peaks appear at 2θ: 21.5° and 54.2°. Meanwhile, the peak that existed before separation persists after separation and there is an increase in intensity. The kaolinite mineral as an impurity in *Mt-clay* also decreased substantially and several peaks experienced a decrease in intensity. Hematite also experiences peak loss. The disappearance of the diffraction peaks of montmorillonite mineral in the *c-Mt-clay* sample calcined at 850°C is due to the dehydroxylation of montmorillonite to meta montmorillonite (Werling *et al.*, 2022). During the calcination process, there is a removal of water from the surface and water between the layers of montmorillonite (Taylor-Lange *et al.*, 2015). This means that montmorillonite undergoes thermal decomposition in the form of dehydration and dehydroxylation during the calcination process (Scrivener and Favier, 2015). According to the XRF results, the Si/Al mole ratio decreased due to the separation and thermal modification processes. A small Si/Al mole ratio indicates a high Al content. High Al comes from aluminate (AlO_4^{5-}) which is negatively charged. The large number of negative

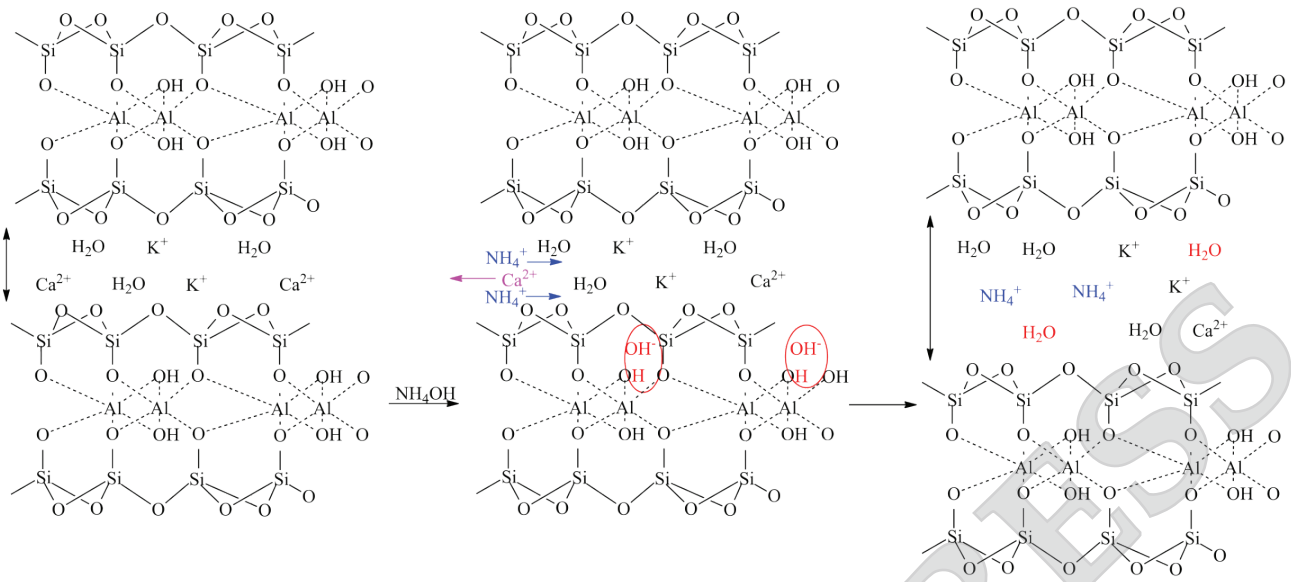

Figure 4. Mechanism of montmorillonite separation using NH_4OH solution.

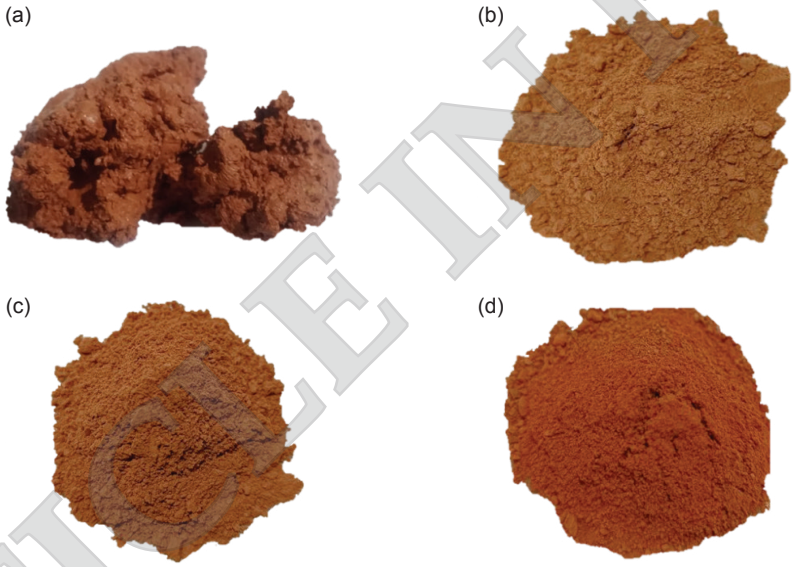

Figure 5. The colour difference of catalyst: a) n-clay, *b)* h-clay, *c)* Mt-clay, *and d)* c-Mt-clay.

charges in the clay mineral layer will increase the electrostatic interaction with the cations in the clay mineral layer (Strawn, 2021). The change in Si and Al levels in clay is caused by isomorphic substitution in the terrestrial sheet (Kukharenko, 1971). Each catalyst also has a good Si / Al mole ratio (1:2) so that the sample can act as a catalyst. If the Si / Al mole ratio is large (>2), the sample will act as an adsorbent.

Effect of Thermal Separation and Modification on the Physical Properties of the Catalyst

Natural clay which is dark brown (*Figure 5a*) and becomes light brown (*Figure 5b, 5c*) in *h-clay* and *Mt-clay*. This is due to the loss of adsorbed water in the clay due to heating at 105°C. The *h-clay* sample is light brown as shown in the figure. The thermal modification also affects the colour of the catalyst. After coking, *c-Mt-clay* turned a brick red colour (*Figure 5d*). The colour change in the clay minerals is due to the transformation of iron oxide contained in each sample. When the clays are calcined in the presence of oxygen at 850°C, goethite [FeO(OH)] transforms into hematite (Fe_2O_3) at 300°C-650°C. Above 650°C, hematite will be reduced to magnetite (Fe_3O_4). However, the samples that have been calcined are cooled again at room temperature. This cooling process will turn magnetite back into hematite. This is what causes the calcined sample to become reddish (Martirena *et al.*, 2020).

Transesterification Reaction Mechanism with Clay Catalyst

The use of each catalyst in the transesterification reaction involves several stages (*Figure 6*). In the first stage, the negatively charged siloxane surface of the clay mineral catalyst skeleton structure can remove H^+ from the hydroxyl group of methanol to form alcohol anion (methoxide) and adsorb on the cation interlayer. When the reaction occurs, the methoxide anion will attack the carbonyl C atom on the triglyceride molecule to form an intermediate. Then, the intermediate undergoes rearrangement by taking H^+ from the siloxane surface to form methyl esters and diglycerides (Intarapong *et al.*, 2014). These stages occur repeatedly so that three moles of methyl ester and one mole of glycerol are formed from one mole of triglyceride.

Differences in Catalytic Activity

The separation and thermal modification of *Mt-clay* and *c-Mt-clay* catalysts can improve catalytic activity (*Figure 7*). The yield of biodiesel in the use of *h-clay* catalyst is 57.67%. The use of *Mt-clay* and *c-Mt-clay* catalysts increased the biodiesel yield to 76.20% and 80.11%, respectively. The increase in catalytic activity is due to the decrease in the Si/Al mole ratio according to the XRF results shown in *Table 1*. The decrease in the Si/Al mole ratio value indicates the increase in Al content of aluminate (AlO_4^{5-}) which is negatively charged so that its electrostatic interaction with cations in the clay mineral interlayer also increases (Strawn, 2021). This shows that the active site of the catalyst also increases so that it can increase its catalytic activity. According to LPSA results, it turns out that particle size does not contribute to catalytic activity. Although it is generally assumed that catalysts with higher surface areas have better activity, this is not always the case. In some cases, the shape and geometry of the catalyst also play an important role in determining its activity (Großmann *et al.*, 2023).

The catalyst produced in this research is more selective than the clay catalyst used by previous researchers (Fifi *et al.*, 2023; Syukri *et al.*, 2022). The *h-clay*, *Mt-clay*, and *c-Mt-clay* catalysts have high selectivity in producing methyl palmitate and methyl oleate. Meanwhile, previous researchers produced various methyl ester products in each biodiesel. The yield of biodiesel produced in this research is also almost the same as previous research (which chemically modified the clay (Fifi *et al.*, 2023; Kansedo *et al.*, 2009). This shows that thermal modification with a simple method and lower cost can also increase the catalytic activity of the montmorillonite mineral.

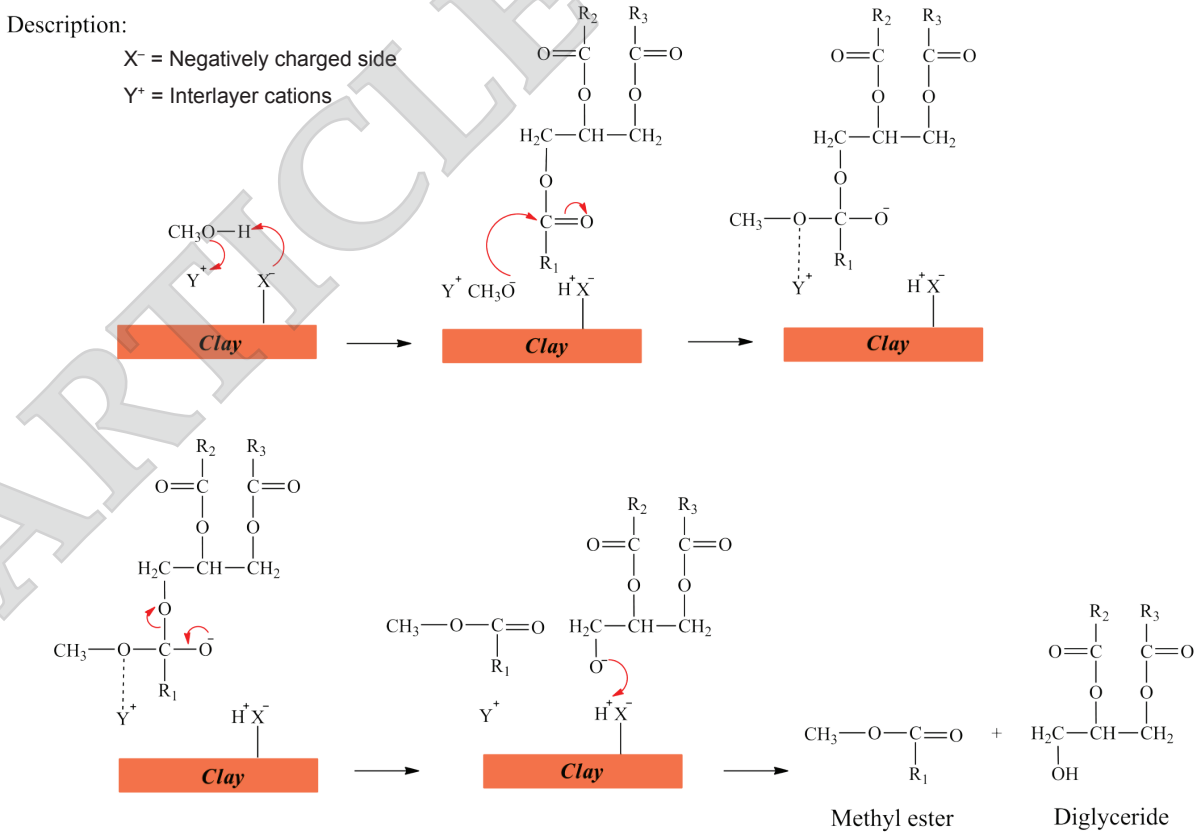

Figure 6. Transesterification reaction mechanism with clay catalysts.

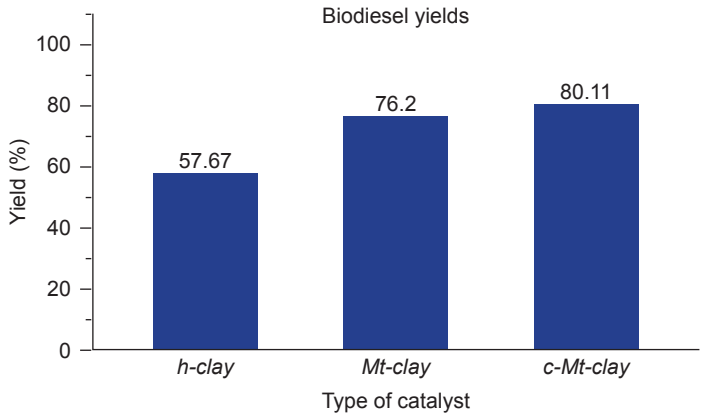

Figure 7. Biodiesel yields catalysed with h-clay, Mt-clay, *and* c-Mt-clay.

TABLE 3. COMPARATIVE STUDY OF MONTMORILLONITE BASED CATALYST ON BIODIESEL YIELD

Catalyst	Feedstock	Temperature (°C)	Time (hr)	Catalyst ratio	Yield (%)	Reference
Cd-Mn-MMT	*Prunus cerasoides* D. oil	120	5	4.0%	85.00	Munir *et al.* (2019)
MMT K10	WCO	150	6	4.0%	38.39	Yahya *et al.* (2020)
Fe-MMT K10	WCO	150	6	4.0%	95.26	Yahya *et al.* (2020)
Nano-MMT	Crude palm oil	60	3	4.0 g	84.90	Harmawan *et al.* (2021)
Copper modified MMT	*Raphnus raphanistrum* L. oil	150	5	3.5%	83.00	Munir *et al.* (2021)
c-Mt-clay	WFO	70	3	3.0%	80.11	This work

TABLE 4. PHYSICAL PROPERTIES OF BIODIESEL CATALYSED BY *h-clay*, *Mt-clay*, AND *c-Mt-clay*

Properties	Standards	Type of catalyst		
		h-clay	*Mt-clay*	*c-Mt-clay*
Density (g cm^{-3})	0.86-0.90 (ASTM D6751)	0.87	0.86	0.86
Water content (%)	0.05 (ASTM D2709)	0.47	0.03	0.02

Transesterification reactions produce similar methyl esters, namely methyl palmitate and methyl oleate. Methyl palmitate is a saturated methyl ester, while methyl oleate is an unsaturated methyl ester. Saturated methyl esters are the most desirable component in biodiesel. This is related to their stability against oxidation. Unsaturated methyl esters, on the other hand, are more easily oxidised and will form gum in the fuel which can cause fuel corrosion (Perosa *et al.*, 2011).

Based on the comparison of montmorillonite-based catalyst studies in the *Table 3*, the yield obtained from this study is higher than the yield obtained in other studies using the MMT K10 synthetic catalyst without treatment and modification. However, when compared with montmorillonite catalysts that were modified by making them nanostructured or by imposition of metal, the yield values obtained in this study were relatively lower.

Physical Properties of Biodiesel Products

The physical properties of the biodiesel product determined are density and water content (*Table 4*). Based on ASTM D6751, biodiesel has a density of 0.86-0.90 g cm^{-3} at 15°C, while the maximum water content in biodiesel is 0.05% (ASTM D2709). The transesterification reaction products catalysed by *h-clay, Mt-clay* and *c-Mt-clay* have densities of 0.87 g cm^{-3}, 0.86 g cm^{-3}, and 0.86 g cm^{-3}, respectively. While the water content in *h-clay, Mt-clay* and *c-Mt-clay* biodiesel products is 0.47%, 0.03% and 0.02%, respectively. Therefore, biodiesel products catalysed by *Mt-clay* and *c-Mt-clay* are included in the biodiesel group because the values meet with the density and water content under ASTM. While the product catalysed by *h-clay* is not considered biodiesel because the water content exceeds the maximum limit set by ASTM.

CONCLUSION

This research has succeeded in separating the mineral montmorillonite from the natural clay of Tanah Datar. Calcined montmorillonite caused changes in the constituent phases, and the element levels, as well as the oxide levels contained therein. All catalysts contain the main elements of Si, Al, and Fe. Separation and thermal modification caused changes in elemental content and Si/Al mole ratio from 1.79 in *h-clay* down to 1.27 and 1.26 in *Mt-clay* and *c-Mt-clay* samples. Thermal treatment of *c-Mt-clay* caused colour changes from light brown to brick red. Montmorillonite turned into meta montmorillonite after calcined at 850°C. Particle size does not contribute to catalytic activity. Separation and thermal modification of *Mt-clay* and *c-Mt-clay* catalysts can increase biodiesel yield. The *h-clay* catalyst had a biodiesel yield of 57.67%, which increased to 76.20% in the *Mt-clay* catalyst and 80.11% in the *c-Mt-clay* catalyst. Therefore, we suggest that other researchers can use this method to produce a good catalyst for producing biodiesel.

ACKNOWLEDGEMENT

We expressed our best gratitude for funding from LPPM Universitas Andalas with Research Contract No. T/174/UN.16.17/PT.01.03/IS-RPT/2022. September 28, 2022.

REFERENCES

Abdrakhimova, E S and Abdrakhimov, V Z (2007). Synthesis of mullite from technogenic materials and pyrophyllite. *Russ. J. Inorg. Chem.*, *52(3)*: 345-350.

Admi, A; Angellika, F T; Rilda, Y and Syukri, S (2022). Pengaruh modifikasi fisika pada komposisi, struktur kristal dan sifat katalitik Lempung Solok. *J. Fis. Unand*, *11(4)*: 548-555.

Azni, M A; Md Khalid, R; Hasran, U A and Kamarudin, S K (2023). Review of the effects of fossil fuels and the need for a hydrogen fuel cell policy in Malaysia. *Sustain.*, *15(5)*: 1-16.

Bambase, M E; Almazan, R A R; Demafelis, R B; Sobremisana, M J and Dizon, L S H (2021). Biodiesel production from refined coconut oil using hydroxide-impregnated calcium oxide by cosolvent method. *Renew. Energy*, *163*: 571-578.

Belghazdis, M and Hachem, E K (2022). Clay and clay minerals: A detailed review. *Int. J. Recent Technol. Appl. Sci.*, *4(2)*: 54-75.

Bibin, C; Gopinath, S; Aravindraj, R; Devaraj, A; Gokula Krishnan, S and Jeevaananthan, J K S (2020). The production of biodiesel from castor oil as a potential feedstock and its usage in compression ignition Engine: A comprehensive review. *Mater. Today Proc.*, *33*: 84-92.

Faruque, M O; Razzak, S A and Hossain, M M (2020). Application of heterogeneous catalysts for biodiesel production from microalgal oil- A review. *Catalysts*, *10(9)*: 1-25.

Febrianto, F; Setianingsih, A and Riyani, A (2020). Determination of free fatty acid in frying oils of various foodstuffs. *Indones. J. Chem. Environ.*, *2(1)*: 1-6.

Fifi, F; Rahmayeni; Admi and Syukri (2023). Kaolinite and illite based clay supporting nickel: Its synthesis, characterization, and catalytic optimazion in a lab-scale fatty acid methyl ester production. *Her. Bauman Moscow State Tech. Univ. Ser. Nat. Sci.*, *4(109)*: 159-174.

Gaide, I; Makareviciene, V; Sendzikiene, E and Kazancev, K (2023). Snail shells as a heterogeneous catalyst for biodiesel fuel production. *Processes*, *11(1)*: 260.

Gautier, M; Muller, F; Le Forestier, L; Beny, J M and Guegan, R (2010). NH_4-smectite: Characterization, hydration properties and hydro mechanical behaviour. *Appl. Clay Sci.*, *49(3)*: 247-254.

Götze, J; Pan, Y and Müller, A (2021). Mineralogy and mineral chemistry of quartz: A review. *Mineral. Mag.*, *85(5)*: 639-664.

Gouran, A; Aghel, B and Nasirmanesh, F (2021). Biodiesel production from waste cooking oil using wheat bran ash as a sustainable biomass. *Fuel*, *295(January)*: 120542.

Großmann, P F; Tonigold, M; Szesni, N; Fischer, R W; Seidel, A; Achterhold, K; Pfeiffer, F and Rieger, B (2023). Influence of internal and external surface area on impregnation and activity of 3D printed catalyst carriers. *Catal. Commun.*, *175*: 106610.

Hamed, N; El-Feky, M S; Kohail, M and Nasr, E S A R (2019). Effect of nano-clay de-agglomeration on mechanical properties of concrete. *Constr. Build. Mater.*, *205*: 245-256.

Harmawan, T; Ani, W; Andani, P and Fadlly, T A (2021). Production of biodiesel through transesterification of crude palm oil (CPO) using montmorillonite nanoparticles (Nano-MMT) as

heterogeneous solid catalyst. *Proc. 2nd Int. Conf. Sci. Technol. Mod. Soc. (ICSTMS 2020)*, *576*: 69-72.

Intarapong, P; Jindavat, C; Luengnaruemitchai, A and Jai-In, S (2014). The transesterification of palm oil using KOH supported on bentonite in a continuous reactor. *Int. J. Green Energy*, *11*: 987-1001.

Irawan, B; Rusdianasari and Hasan, A (2021). Pyrolysis process of fatty acid methyl ester (FAME) conversion into biodiesel. *Int. J. Res. Vocat. Stud.*, *1(2)*: 1-10.

Jabbari, H (2018). Production of methyl ester biofuel from sunflower oil via transesterification reaction. *Asian J. Nanosci. Mater.*, *1(2)*: 52-55.

Kansedo, J; Lee, K T and Bhatia, S (2009). Biodiesel production from palm oil via heterogeneous transesterification. *Biomass Bioenergy*, *33(2)*: 271-276.

Khan, E; Ozaltin, K; Spagnuolo, D; Bernal-Ballen, A; Piskunov, M V and Di Martino, A (2023). Biodiesel from rapeseed and sunflower oil: Effect of the transesterification conditions and oxidation stability. *Energies*, *16(2)*: 1-13.

Kibar, M E; Hilal, L; Çapa, B T; Bahçıvanlar, B and Abdeljelil, B (2023). Assessment of homogeneous and heterogeneous catalysts in transesterification reaction: A mini review. *ChemBioEng Rev.*, *10(4)*: 412-422.

Kukharenko, A A (1971). The problem of isomorphism in mineralogy. *Int. Geol. Rev.*, *13(4)*: 546-557.

Lomertwala, H M; Njoroge, P W; Opiyo, S A and Ptoton, B M (2019). Characterization of clays from selected sites for refractory application. *Int. J. Sci. Res. Publ.*, *9(11)*: p9581.

Lugo-Méndez, H; Sánchez-Domínguez, M; Sales-Cruz, M; Olivares-Hernández, R; Lugo-Leyte, R and Torres-Aldaco, A (2021). Synthesis of biodiesel from coconut oil and characterization of its blends. *Fuel*, *295(1)*: 120595.

Martirena, F; Almenares, R; Zunino, F; Alujas, A and Scrivener, K (2020). Color control in industrial clay calcination. *RILEM Tech. Lett.*, *5*: 1-7.

Mishra, V K and Goswami, R (2018). A review of production, properties and advantages of biodiesel. *Biofuels*, *9(2)*: 273-289.

Munir, M; Ahmad, M; Waseem, A; Zafar, M; Saeed, M; Wakeel, A; Nazish, M and Sultana, S (2019). Scanning electron microscopy leads to identification of novel nonedible oil seeds as energy crops. *Microsc. Res. Tech.*, *82(7)*: 1165-1173.

Munir, M; Ahmad, M; Rehan, M; Saeed, M; Lam, S S; Nizami, A S; Waseem, A; Sultana, S and Zafar, M (2021). Production of high quality biodiesel from novel non-edible *Raphnus raphanistrum* L. seed oil using copper modified montmorillonite clay catalyst. *Environ. Res.*, *193*: 110398.

Mustafa, N; Zubair, M; Uddin, N; Ali, S; Haider, A and Badshah, A (2023). Catalytic conversion of castor oil into biodiesel by tri-organotin(iv) catalysts: Chromatographic and spectroscopic characterization with theoretical support. *Proc. Pakistan Acad. Sci. Part B*, *60(2)*: 225-232.

Nang, H L L; Wafti, N S A and May, C Y (2009). Production technology of biodiesel from palm fatty acid distillate (PFAD). *MPOB Inf. Ser.*, *471(4)*.

Negm, N A; Sayed, G H; Yehia, F Z; Habib, O I and Mohamed, E A (2017). Biodiesel production from one-step heterogeneous catalyzed process of Castor oil and *Jatropha* oil using novel sulphonated phenyl silane montmorillonite catalyst. *J. Mol. Liq.*, *234*: 157-163.

Nguyen, V G; Pham, M T; Le, N V L; Le, H C; Truong, T H and Cao, D N (2023). A comprehensive review on the use of biodiesel for diesel engines. *Int. J. Renew. Energy Dev.*, *12(4)*: 720-740.

Pacheco-López, A; Lechtenberg, F; Somoza-Tornos, A; Graells, M and Espuña, A (2021). Economic and environmental assessment of plastic waste pyrolysis products and biofuels as substitutes for fossil-based fuels. *Front. Energy Res.*, *9*: 1-14.

Palaniselvam, V; Rajan, S S; Sriramajaman, S and Ramesh, D (2023). Effect of reaction time on various properties of palm oil biodiesel in continuous biodiesel reactor. *J. Oil Palm Res.* DOI: 10.21894/jopr.2023.0040.

Park, J H; Shin, H J; Kim, M H; Kim, J S; Kang, N; Lee, J Y; Kim, K T; Lee, J I and Kim, D D (2016). Application of montmorillonite in bentonite as a pharmaceutical excipient in drug delivery systems. *J. Pharm. Investig.*, *46(4)*: 363-375.

Pasae, Y; Melawaty, L; Ruswanto; Bulo, L and Allo, E L (2021). Effectiveness of heterogenous catalyst in biodiesel production process: The use of zeolite, ZnO and Al_2O_3. *J. Phys. Conf. Ser.*, *1899(1)*: 1-6.

Peng, C; Wang, G; Qin, L; Luo, S; Min, F and Zhu, X (2020). Molecular dynamics simulation of NH_4-montmorillonite interlayer hydration: Structure,

energetics, and dynamics. *Appl. Clay Sci.*, *195*: 105657.

Perosa, A; Selva, M; Lucchini, V; Fabris, M and Noè, M (2011). Kinetic parameter estimation of solvent-free reactions monitored by 13C NMR spectroscopy, a case study: Mono- and di-(hydroxy)ethylation of aniline with ethylene carbonate. *Int. J. Chem. Kinet.*, *43(3)*: 154-160.

Pikula, K; Zakharenko, A; Stratidakis, A; Razgonova, M; Nosyrev, A; Mezhuev, Y; Tsatsakis, A and Golokhvast, K (2020). The advances and limitations in biodiesel production: Feedstocks, oil extraction methods, production, and environmental life cycle assessment. *Green Chem. Lett. Rev.*, *13(4)*: 11-30.

Rehman, A; Ma, H; Chishti, M Z; Ozturk, I; Irfan, M and Ahmad, M (2021). Asymmetric investigation to track the effect of urbanization, energy utilization, fossil fuel energy and CO_2 emission on economic efficiency in China: Another outlook. *Environ. Sci. Pollut. Res.*, *28(14)*: 17319-17330.

Salaheldeen, M; Mariod, A A; Aroua, M K; Rahman, S M A; Soudagar, M E M and Fattah, I M R (2021). Current state and perspectives on transesterification of triglycerides for biodiesel production. *Catalysts*, *11(9)*: 1-37.

Scrivener, K and Favier, A (2015). *Calcined Clays for Sustainable Concrete*. RILEM Bookseries. p. 117-124.

Shapkin, N P; Leont'ev, L B; Khal'chenko, I G; Panasenko, A E; Maiorov, V Y; Razov, V I; Kaidalova, T A and Papynov, E K (2017). Chemical modification of natural clays. *Russ. J. Inorg. Chem.*, *62(9)*: 1209-1214.

Sharma, P and Bhavani, A G (2021). Green, cost effective barium loaded montmorillonite catalyst for biodiesel synthesis from waste cooking oil. *Mater. Today Proc.*, *45*: 4544-4549.

Siddeg, A B; Adam, U; Jaat, N; Khalid, A; Sapit, A; Mohd, S and Abd. Jalal, M (2022). Analysis of the influences of biodiesel on performance and emissions of a diesel engine. *J. Automot. Powertrain Transp. Technol.*, *2(2)*: 1-8.

Silva, A A de L; Periera, M G A; Souza, L Di and Caldeira, A G D S (2015). Iodeto de potássio suportado em MCM-41 como catalisador para síntese de biodiesel utilizando micro-ondas. *Blucher Chemi. Proc.* p. 537-545.

Strawn, D G (2021). Sorption mechanisms of chemicals in soils. *Soil Syst.*, *5(1)*: 1-22.

Sukkathanyawat, H and Wichianwat, K (2023). Optimisation of FAME production from waste cooking palm oil with KOH catalyst supported on palm kernel shells ash (PKSA) using response surface methodology (RSM). *J. Oil Palm Res.*, *35(4)*: 668-681.

Supriyanto, E; Sentanuhady, J; Dwiputra, A; Permana, A and Muflikhun, M A (2021). The recent progress of natural sources and manufacturing process of biodiesel: A review. *Sustain.*, *13(10)*: 5599.

Suwarno; Rohana and Indra Siregar, I (2021). Study feasibility analysis of biodiesel energy processing used cooking oil. *Budapest Int. Res. Critics Inst. J.*, *4(3)*: 7374-7386.

Syukri; Fifi, F; Rahmayeni; Mai, E; Eka, P Y and Upita, S (2022). Effect of thermal treatment and nickel-salt modification on the catalytic performance of the illite-kaolinite clay from Bukittinggi of West Sumatra in palm oil transesterification. *Her. Bauman Mosc. State Tech. Univ. Ser. Nat. Sci.*, *2*: 125-136.

Syukri, S; Septioga, K; Arief, S; Putri, Y E; Efdi, M and Septiani, U (2020). Natural clay of Pasaman Barat enriched by CaO of chicken eggshells as catalyst for biodiesel production. *Bull. Chem. React. Eng. Catal.*, *15(3)*: 662-673.

Takabatake, M and Motokura, K (2022). Montmorillonite-based heterogeneous catalysts for efficient organic reactions. *Nano Express*, *3(1)*: 014004.

Taslimah; Kusumawardani, R and Azmiyawati, C (2008). Pilarisasi lempung dengan Al_2O_3 untuk agen pemucat minyak sawit. *J. Sci. Appl. Chem.*, *11(2)*: 48-51.

Taylor-Lange, S C; Lamon, E L; Riding, K A and Juenger, M C G (2015). Calcined kaolinite-bentonite clay blends as supplementary cementitious materials. *Appl. Clay Sci.*, *108*: 84-93.

Tong, K; Guo, J; Chen, S; Yu, F; Li, S and Dai, Z (2021). A simulation study on the swelling and shrinking behaviors of nanosized montmorillonite based on Monte Carlo and molecular dynamics. *Geofluids*, *2021*: 1038205.

Tripol'Skaya, T A; Pilipenko, G P; Legurova, E A; Pokhabova, I V and Prikhodchenko, P V (2009). New peroxo derivatives of synthetic montmorillonite structures. *Russ. J. Inorg. Chem.*, *54(4)*: 512-516.

Ubaid, H S; Noureen, S; Razzaq, I; Alkhter, S; Mehmood, F; Razzaq, Z and Jabeen, M (2022). Optimisation and characterisation of acid catalysed

castor biodiesel and its blends. *J. Turkish Chem. Soc. Sect. A Chem.*, *9(4)*: 1007-1022.

Uddin, F (2018). Montmorillonite: An introduction to properties and utilization. *Current Topics in the Utilization of Clay in Industrial and Medical Applications* (Zoveidavianpoor, M eds.). IntechOpen. London. 202 pp.

Vital-López, L; Mercader-Trejo, F; Rodríguez-Reséndiz, J; Zamora-Antuñano, M A; Rodríguez-López, A; Esquerre-Verastegui, J E; Farrera Vázquez, N and García-García, R (2023). Electrochemical characterization of biodiesel from sunflower oil produced by homogeneous catalysis and ultrasound. *Processes*, *11(1)*: 1-12.

Werling, N; Kaltenbach, J; Weidler, P G; Schuhmann, R; Dehn, F and Emmerich, K (2022). Solubility of calcined kaolinite, montmorillonite, and illite in high molar NaOH and suitability as precursors for geopolymers. *Clays Clay Miner.*, *70(2)*: 270-289.

Wu, Z; Zhao, H; Zhou, X; Wang, Y; Zuo, K and Cheng, H (2022). Thermal migration behavior of Na^{+}, Cu^{2+} and Li^{+} in montmorillonite. *Minerals*, *12(4)*: 477.

Xu, H; Ou, L; Li, Y; Hawkins, T R and Wang, M (2022). Life cycle greenhouse gas emissions of biodiesel and renewable diesel production in the United States. *Environ. Sci. Technol.*, *56(12)*: 7512-7521.

Yaghmaeiyan, N; Mirzaei, M and Delghavi, R (2022). Montmorillonite clay: Introduction and evaluation of its applications in different organic syntheses as catalyst: A review. *Results Chem.*, *4*: 100549.

Yahya, S; Muhamad Wahab, S K and Harun, F W (2020). Optimization of biodiesel production from waste cooking oil using Fe-Montmorillonite K10 by response surface methodology. *Renew. Energy*, *157*: 164-172.